

2021

Backfill grouting for mining subsidence prevention

Habib Alehossein
CSIRO Mineral Resources

Baotang Shen
University of Queensland

Zongyi Qin
University of Queensland

Follow this and additional works at: <https://ro.uow.edu.au/coal>

Recommended Citation

Habib Alehossein, Baotang Shen, and Zongyi Qin, Backfill grouting for mining subsidence prevention, in Naj Aziz and Bob Kininmonth (eds.), Proceedings of the 2021 Resource Operators Conference, Mining Engineering, University of Wollongong, 18-20 February 2019
<https://ro.uow.edu.au/coal/800>

Research Online is the open access institutional repository for the University of Wollongong. For further information contact the UOW Library: research-pubs@uow.edu.au

BACKFILL GROUTING FOR MINING SUBSIDENCE PREVENTION

Habib Alehossein¹, Baotang Shen² and Zongyi Qin²

ABSTRACT: Mining subsidence has been a major hazard in most underground coal mines, particularly those where designs and practices are based on the wrong assumption of fixed, permanent and nondeteriorating coal pillars. Mining induced subsidence significantly affects mining costs where major surface structures and natural environment need to be protected. Remedial measures to manage damage caused by subsidence can often be very costly with potentially damaging impacts and irreversible consequences. Backfilling and injection of granular materials into the mining induced voids, separated beddings and cracks, as either diluted granular slurry or concrete paste, is widely used to control mine subsidence overseas. Granular grouts and slurries made of mine and power plant wastes and rejects are viable environmental backfill solutions to both ground stability and mine waste management problems. Like concrete paste, the flowing slurry can be categorised as a generally nonlinear frictional viscous cohesive (Bingham Herschel-Bulkley) fluid. The general frictional viscous, cohesive, non-Newtonian fluid model has been applied to concrete flowability problems such as L-box and slump tests. While slump test is used in shallow foundations, L-box test is used in difficult deep foundations. It is designed to measure workability and flowability of tremie pipe concrete as an indirect index measure of concrete viscosity and plastic yield. Tremie pipes are used to control concrete flow rate and minimise bleeding and dilution when placed into deep submerged excavations. Mathematical and experimental models have been developed to not only solve the flow velocity along the L-box channel length as a function of time and distance, but also simulate the flow of the backfill material and demonstrate the detailed process of filling the voids to minimise any further subsidence.

INTRODUCTION

Mining Subsidence

As a major potential hazard, mining induced subsidence significantly affects mining costs where major surface structures and natural environment need to be protected, e.g. mining under river systems, gorges, cliffs, power lines, pipelines, communication cables, major roads and bridges, and other significant surface facilities. Remedial measures to manage damage caused by subsidence can often be very costly with potentially damaging impacts and irreversible consequences. The recent mining induced subsidence events occurred at Collingwood Park of Ipswich (Figure 1) are great cases of unforeseen risk, how easily material strength can deteriorate and result in surface ground subsidence, and severe consequences in mine safety, stability, accessibility and reliability (Shen et al, 2010).

Backfilling and injection of granular materials into the mining induced voids, separated beddings and cracks, as either diluted granular slurry or concrete paste, is widely used to control mine subsidence. Granular grouts and slurries made of mine and power plant wastes and rejects are viable environmental backfill solutions to both ground stability and mine waste management problems. Like concrete paste, the flowing slurry can be categorised as a generally nonlinear frictional viscous cohesive (Bingham Herschel-Bulkley) fluid (Alehossein, 2009, Alehossein et al, 2012). However, in mining applications, to reduce ground surface subsidence and control the propagation of the overburden movement to the surface, the solid particles in the injected slurry must deposit in the bed separation gaps of the coal seam over-burden strata, e.g. in longwall mining the grout slurry is pumped into the separated beds of the rock mass from a batching plant source through pipelines connected to a central vertical borehole, which is drilled deep into the over-burden rock above the coal seam (Alehossein and Poulsen, 2010). Flow blockage can occur in the injection system, when the

¹ Mineral Resources, Commonwealth Scientific and Research Organisation (CSIRO), Email: baotang.shen@csiro.au Tel: +61 7 3327 4560

² Mining Program, University of Southern Queensland (USQ), Email: habib.alehossein@usq.edu.au Tel: +61 7 4631 1390

slurry velocity falls below a certain critical threshold velocity. The stiffening, consolidating non-flow slurry can generally be categorised as a frictional cohesive soil (Shen, and Alehossein, 2009). In other words, a change of material phase from cohesive-viscous to cohesive-frictional will occur. Using a smaller scale model, this field injection practice has been simulated at the QCAT laboratory of CSIRO in Brisbane, Australia, to study the influence of various grout injection parameters by pumping slurries through various pipes of different sizes and diameters and for different applications (Alehossein 2009). As an important industrial application, grout injection into the inter-burden strata is used as a modern technology to control and reduce coal mine subsidence. Slurry mixes of coal mine and power plant waste materials, e.g. fly ash or any other coal wash rejects, are injected back into the inter-burden rock strata during longwall mining. To reduce subsidence and control inter-burden strata movement, the injected slurry solid particles must deposit in the opened strata bed separation gaps or cracks before crack closure. The mechanics of non-Newtonian fluids flowing between parallel disks is a classical fluid mechanics problem that has been studied by a number of researchers in the past for their specific problems of interest (Beckhaus, et al, 2011, 2012, Qin et al, 2013, Larisch et al, 2013). Tremie pipes are used to control concrete flow rate and minimise bleeding and dilution when placed into deep submerged excavations. The L-box test is designed to measure workability and flowability of tremie pipe concrete as an indirect index measure of concrete viscosity and plastic yield. The L-box model solves a dimensionless PDE in terms of the flow velocity along the L-box channel length as a function of time and distance, which is analogous to a non-homogeneous heat conduction equation. The general frictional viscous, cohesive, non-Newtonian fluid model has been applied to concrete flowability problems such as L-box and slump tests. Figure 2 shows applications of this modelled fluid in concrete L-Box tests (Left), injection into strata (Middle) and laboratory scale-down injection experiments (Right).



Figure 1: Locations of 15 drill holes designed by CSIRO distributed in both historical subsided and non-subsided areas (Shen et al, 2010)

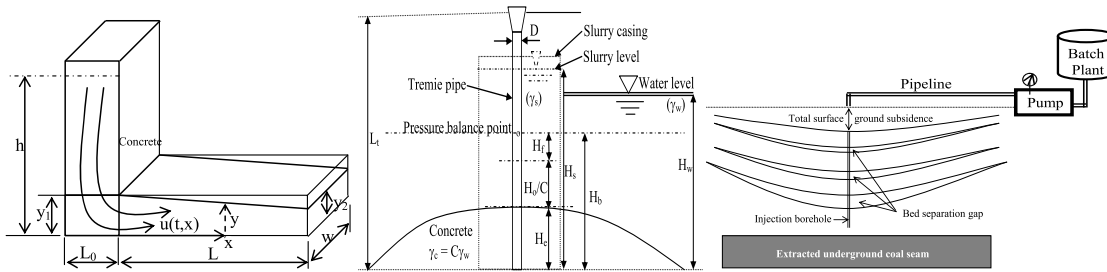


Figure 2: Various applications of viscous slurry and paste fluids: (a) channel flow for workability and consistency testing of concrete; (b) Concrete tremie pipe flow into submerged foundations; (c) multi-phase slurry flow in pipes and fractured rock strata for void backfilling

Pillar Failure

In the room and pillar mining method, the overburden load must be carried by the coal pillars left in the coal seam with the danger of failure due to many possible mechanisms such as coal weathering and deterioration due to the lack of confinement or erosion by flooding, or close proximity to the natural fault zones. Figure 3 shows the 3D seismic results of the amplitude distribution of seam reflections when mapping failure in the coal seam. It clearly shows that the subsidence area on the surface and failure area at the seam level are different.

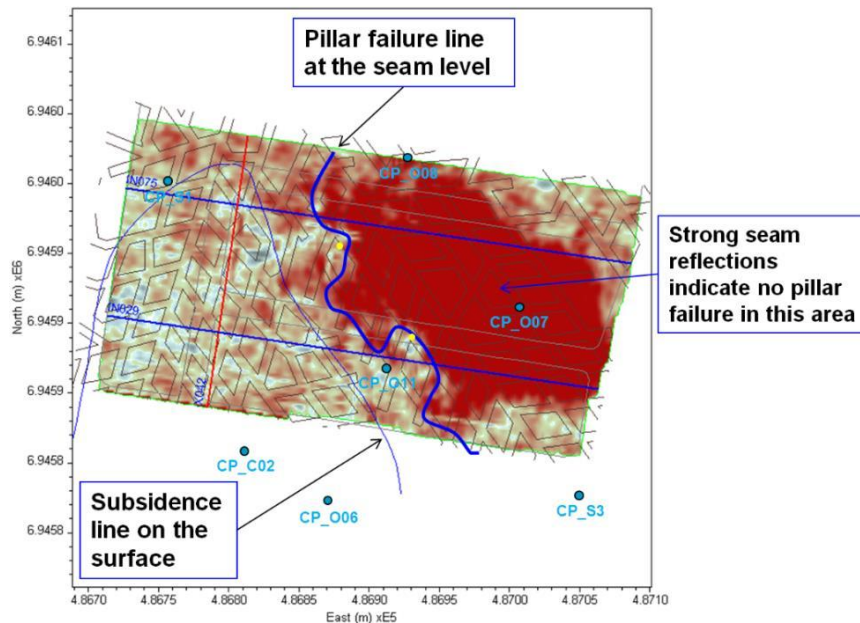


Figure 3: 3D seismic results. Amplitude distribution of seam reflections for mapping the failure at the seam level. Yellow dots are the failure boundary locations at the seam level mapped from seismic sections. Thick blue curve describes the failure boundary at the seam level based on the reflection amplitude strength. Light blue dots are the boreholes drilled after the 3D seismic field work (Shen et al, 2010)

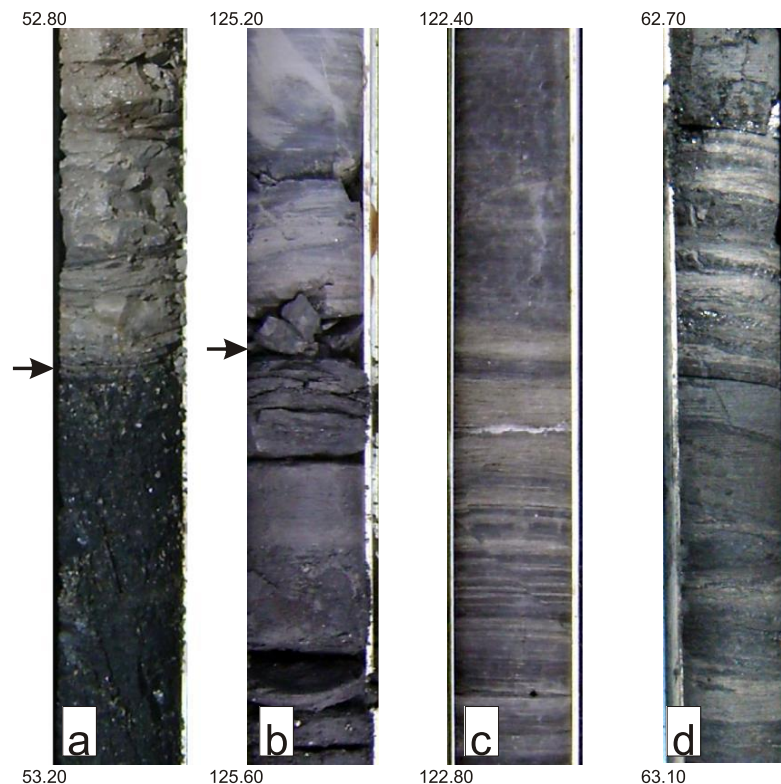
The thick blue line is the failure boundary locations at the seam level mapped from specified seismic sections. The thick blue curve describes the failure boundary at the seam level based on the reflection amplitude strength. Amplitudes are clipped to make the selection of the subsidence boundary at the seam level easier. The light blue dots are the boreholes drilled after the 3D seismic field work. Using

fly ash and mine slurry wastes, various backfill mixes were investigated as a mitigation solution to the prevention of further subsidence.

LITHOLOGIES

Blackstone Formation

The Blackstone Formation consists of coal, interbedded shale, siltstone and fine sandstone (Figure 4), and has been interpreted as being deposited in a fluvial environment with floodplains, meandering channels and peat forming mires (Shen et al. 2010). This environment results in stratigraphy that has a high degree of lateral variation. For example, the two seams that make up the Main Seam, the Bluff and Four Foot Seams, are separated by tens of metres of interburden elsewhere in the basin, whereas they are in contact in the study area. There are numerous clay bands (tonsteins) in the formation that have been interpreted as volcanic ash falls. Where drilled, the floor of the Main Seam (CP_C01, CP_C02, CP_O11, DME BH2) consists of siltstone and carbonaceous mudstone (Figure 3). The top of the Main Seam has been eroded by the overlying Aberdare Conglomerate in the Westfalen No. 3 area. Recent drilling suggests that this overlying unit is several metres above the roof of the Main seam throughout most of the mine area, and that the seam is largely intact (Shen et al, 2010). The immediate roof of the coal seams consists of fine grained sandstone thinly interbedded with siltstone and carbonaceous mudstone and appear to conformable with the coal in CP_C01, CP_C03 and DEM



BH2. These sediments are interpreted to be part of the Blackstone Formation.

Figure 4: Lithologies from the Blackstone Formation. a) top of the Main Seam in CP_C01, b) top of the main seam in CP_C03, c) interbedded fine sandstone, siltstone and carbonaceous mudstone in the roof of the Main Seam (CP_C03), and d) interbedded siltstone, carbonaceous mudstone and coal bands in the floor of the Main Seam (CP_C01), (Shen et al, 2010)

Backfilling Remediation

Using fly ash and mine slurry wastes, various backfill mixes were investigated as a mitigation solution to the prevention of further subsidence. The freely available fly ash was a good candidate in this

investigation. A scale-down model of the mine and pillars was developed at the CSIRO laboratory which were then filled with various fly ash slurries. These experiments proved suitability of fly ash for successful deposition, sedimentation and consolidation of the backfill and its subsidence prevention application, as shown in Figure 5. These laboratory and field experiments on mine-backfill fluids, slurries, cements, pastes and concretes proved their wide range of shear resistance and complex behaviour in response to shearing necessitating development of a general, nonlinear, cohesive, viscous, frictional, nonlinear, non-Newtonian model of shear stress versus shear strain rate, as an extension to the classical Bingham-Herschel-Bulkley fluid. The value of the shear strength function at zero shear strain rate, i.e. plastic yield and the tangent slope of the stress-strain rate curve (viscosity), at any given shear rate, are the two most important parameters of such fluids – Figure 5.

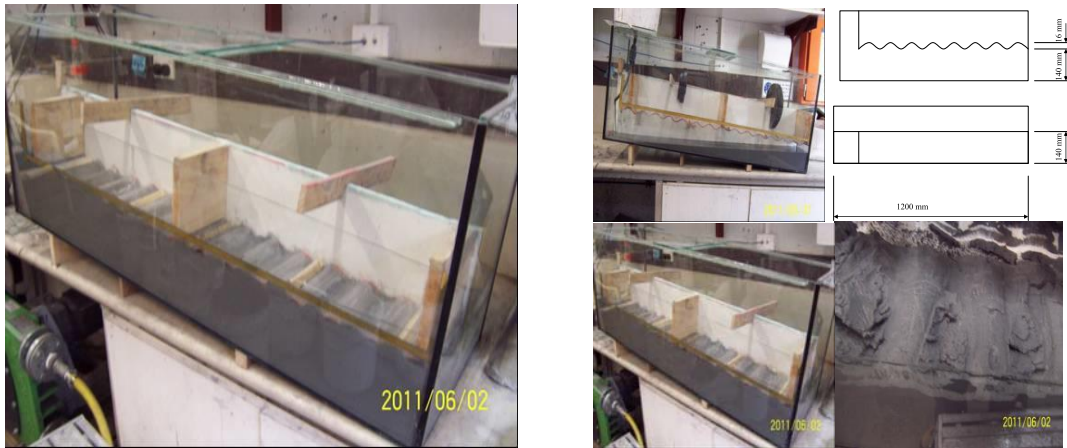


Figure 5: Laboratory scale-down simulation of mine backfill using mixtures of fly ash being deposited in the simulated mine prototype

FRICIONAL VISCOPLASTIC FLUID MECHANICS ANALYTICAL SOLUTIONS

Referring to Figure 6 (left), the general constitutive equation, relating fluid shear stress to shear rate for such general nonlinear, non-Newtonian, viscous, plastic, frictional fluids, which can be applied to fresh concrete, mine backfill slurries and high frictional multiphase fluids, is as follows (Alehossein, 2009)

$$\tau(t, \mathbf{x}) = \mu(t, \mathbf{x}) \left(-\frac{\partial \mathbf{u}(t, \mathbf{x})}{\partial \hat{\mathbf{x}}} \right) + \eta(t, \mathbf{x}) \left(-\frac{\partial \mathbf{u}(t, \mathbf{x})}{\partial \hat{\mathbf{x}}} \right)^n + \tau_0(t, \mathbf{x}) + \xi(t, \mathbf{x}) p(t, \mathbf{x}) \quad (1)$$

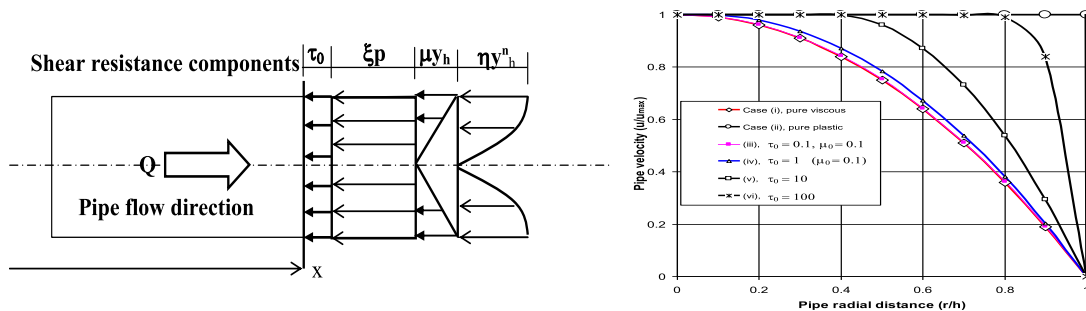


Figure 6: Various shear stress components of Equation (1) (LHS) and its applications (RHS)

In Equation (1) τ is shear stress tensor, \mathbf{u} is velocity vector, μ and η are linear and nonlinear viscosities, τ_0 is plastic yield, p is pipe pressure and ξ is concrete friction coefficient. The last term, involving the friction and pressure terms (ξ_p), is a frictional resistance term which can be applied only

when a pipe blockage occurs due to the concrete granular material friction and needs to be reopened by a higher pressure flow, otherwise it can be ignored. Various shear stress components are shown in the left hand side of Figure 6, where τ_0 is the constant uniform plastic yield component, with no viscosity; μ is the Newtonian linear viscosity coefficient of the linear velocity gradient y with a wall value y_h ; η is the non-linear viscosity; ξ is the friction coefficient of the fluid pressure p . Right hand side of Figure 6 shows the comparisons of normalised velocity profiles for different slurries of various viscosity (μ) and plasticity (τ) in a pipe flow.

Exact equations can be derived to relate the fluid flow rate Q to the fluid pressure p , e.g. in a pipe or radial disc. The results are integral equations relating velocity gradient y , or y_h (or ψ , or ψ_h in the case of radial flow) to the flow rate Q (Alehossein 2009, Alehossein, et al 2012).

$$\text{Pipe Flow: } Q = \int_A \bar{u} \cdot d\bar{A} = 2\pi \int_0^h x_2 u_1 dx_2 = \frac{\pi}{3} h^3 (y_h - F_h^{-3} G_h) \quad (2a)$$

$$\text{Radial Flow: } Q = \int_A \bar{u} \cdot d\bar{A} = 2\pi \int_0^h x_2 u_1 dx_2 = 2\pi h^2 (\psi_h - f_h^{-2} g_h) \quad (2b)$$

Slurry flow may be assumed to stop in the case of a blockage ($Q \rightarrow 0$), which means the boundary values of the velocity gradients y_h and $g(y_h)$ are identically zero. This is due to the effects of the cohesive frictional terms (τ and τ_0) introduced in the shear stress Equation (1), which now become dominant in blocking the slurry flow. The above general theory is certainly reducible to simpler classical Newtonian and Bingham models with appropriate parameter substitutions, as demonstrated by separated components in Figure 6 (Left).

EXPERIMENTS

L-Box Test

L-box test is a relatively new laboratory and on-site testing method to check whether or not a fresh tremie concrete with a maximum coarse aggregate size (e.g. 20 mm) or less is able to flow into all spaces within a foundation excavation and through tight small spaces and openings under a certain concrete head (Beckhaus et al, 2011).

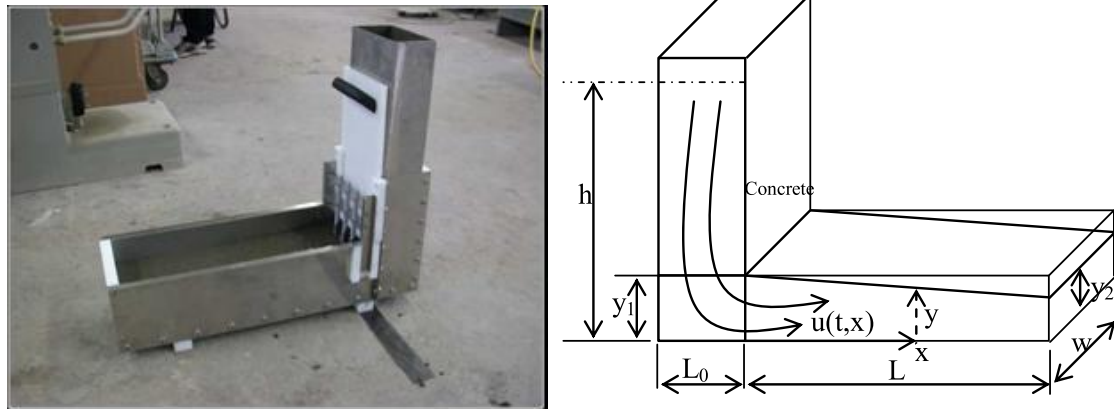


Figure 7: An L-box test gear (left) for measuring visco-plastic behavior of fresh concrete samples by pouring concrete into the vertical rectangular chimney box and let it flow into the horizontal channel box by opening a sliding gate attached to the chimney box. Flow time (T_0) and end heights of concrete flow profile (y_1, y_2) are measured (Beckhaus et al, 2011)

A photo of the L-box test is shown in the left hand side of Figure 7, with schematic size details on the right hand side figure. A sample of a concrete of certain weight is placed into the vertical rectangular chimney of the L-box first, then, the vertical sliding gate attached to the chimney part is opened to

allow the concrete flow horizontally. Both the time (T_0), which takes the concrete to reach the other end, and the end profile coordinate, y_2 , are measured. As an example: $L_0 = 3.94$ in [100 mm], $L = 27.56$ in [700 mm], $h = 23.62$ in [600 mm], $W = 7.87$ in [200 mm], $y_1 = 5.91$ in [150 mm], $y_2 = 2.95$ in [75 mm], time for complete flow reaching the other end T_0 is less than 10 seconds.

Concrete flow during pouring and flowing in channels, chutes and testing equipment for testing purposes are normally not at a steady state situation. General time-dependent 2D and 3D differential equations governing flow of concrete in rectangular channels and chutes can be developed and solved numerically, as shown in (Alehossein et al 2012). However, for the sake of understanding, it is also possible to reduce these equations to a simple 1D form, based on an assumption that there is no significant independent variation in any variable or function in the normal directions x_2 and x_3 compared to the longitudinal main flow direction x_1 . In other words,

$$\tau_{,x_2}(t, x_1) - p_{,x_1}(t, x_1) - \rho u_{,t}(t, x_1) = 0 \quad (3)$$

which gives a solution in terms of Fourier coefficients

$$u(t, x) = \sum_{n=0}^{\infty} e^{-a\kappa_n^2 t} (A_n \cos(\kappa_n x) + B_n \sin(\kappa_n x)) + mx^2 \quad (4)$$

In the solution (4) κ is an arbitrary constant satisfying both the differential equation and the boundary conditions, while A_n and B_n are Fourier coefficients to be determined from the boundary conditions. Figure 8 shows a typical result for various values of n truncating the number of Fourier terms. It shows results of the Fourier analysis for the two cases of $u(0, x)$ and $u(0.5, x)$, and the increasing effects of the number of Fourier terms, namely from $n = 5, 10$ to 120 . The second line in the figure corresponds to velocity at time $t = 0.5$ for different profile points along the x line using $n = 120$. Notice that since continuity and differentiability is not a requirement at the end points of a Fourier series analysis (Alehossein et al 2012), it doesn't converge to the numerical solution at point $x = 1$, as expected.

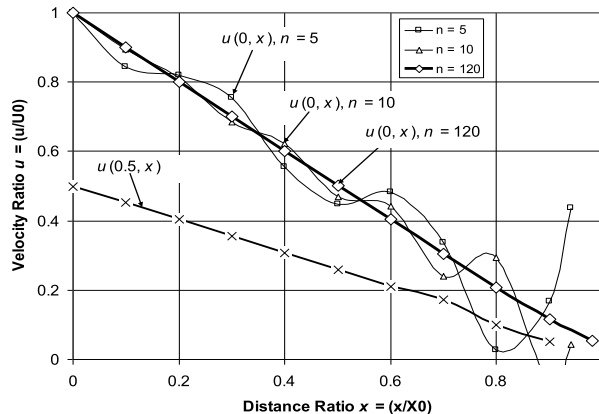


Figure 8: The function $u(0, x)$ represented by a Fourier series with different number of Fourier coefficients: $n = 5, 10, 120$ (Alehossein et al, 2012)

CFD NUMERICAL SIMULATIONS

Computational fluid dynamics (CFD) simulations of the concrete tests, e.g. slump and L-box tests, can be carried out to predict the flow-ability and stability of real fresh concretes, e.g. tremie pipe concretes placed in deep and underground pile foundations. Concrete placement in piles is a blind process, especially for deep foundation elements. To control the quality of the foundation, it is desirable to know the concrete flow performance during placement. The advance of CFD provides the possibility to simulate the whole process of pouring concrete in the deep excavation or cavity in a soil or rock mass. With the aid of graphs or videos of the results, the simulation allows engineers to virtually “see” what is happening in the inaccessible space where the concrete is flowing. Before simulating the real concrete placement process, small scale model tests need to be established to simulate the laboratory test and validate the numerical model.

Two CFD models are developed to simulate slump and L-box tests. Each model mimics the same geometry as required by the real slump and L-box tests, as described previously. The geometrical models used for CFD discretisation (mesh) are shown in Figure 9. The multiple material phase models (concrete, water, air) are used in the CFD modeling. Flow behaviour in the two tests is treated as transient. The concrete mix is treated as a non-Newtonian frictional viscoplastic fluid (2-4). For the L-box test, the concrete stays initially in the vertical section of the L-box, i.e. the horizontal section of the L-box is initially empty. The concrete starts to flow due to gravity when the gate opens or will be removed. For the slump test, the initial condition is that the test cone is fully filled with concrete. The simulation starts when the cone is lifted or removed. Figure 9 displays the process of the tremie concrete flowing along the L-box. The flow length, represented by the distance from the gate to the tip of the concrete is recorded, as shown in Figure 10. It can be seen that the tip of the concrete reached the end of the horizontal box at about $t = 8$ s, which matches the real test results. In addition to the concrete flow profiles and profile fractions, CFD method can provide many other features and information about the flow performance such as pressure, velocity and temperature at any time and any location.

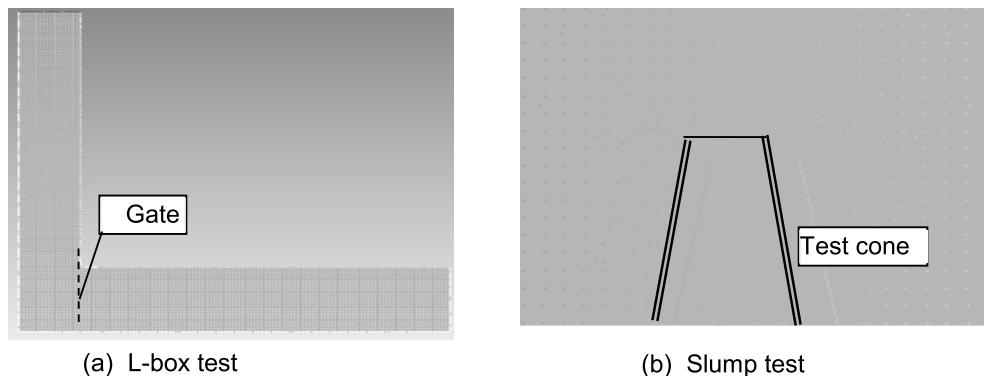


Figure 9: Meshed geometries of CFD models for the slump test and the L-box test

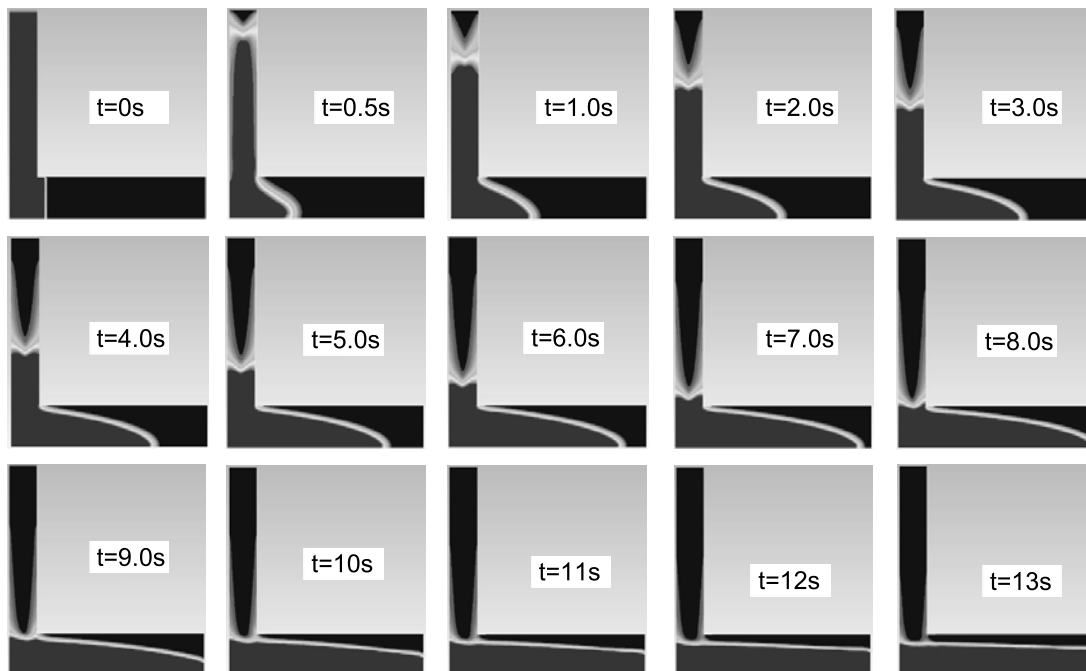


Figure 10: CFD simulated process of the L-box test showing the fraction of concrete in the modelled domain

Figure 11 shows the CFD modelling results of the familiar concrete slump test world widely used. The initial condition is that the test slump cone is fully filled with concrete and the simulation starts when the cone is lifted or removed. In this figure, the maximum CFD drop and spread are 252 and 410mm matching well an experimental test result (Larisch et al, 2013).

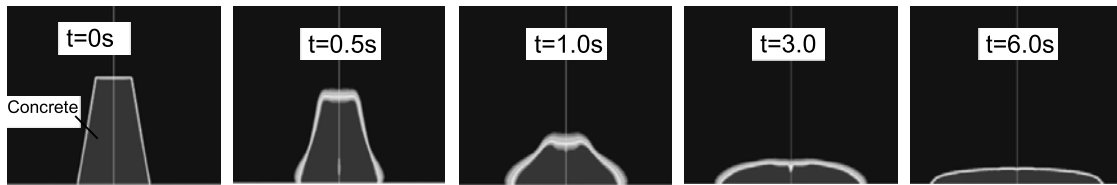


Figure 11: CFD simulation of concrete slump test at different times

CONCLUSIONS

Experimental and numerical (CFD) simulations carried out proved that both slurry backfills and modern concrete can be modelled as a non-Newtonian frictional viscoplastic Bingham-plastic fluid. The CFD simulations demonstrated that the method is capable of shedding light on the “blind process” side of concreting deep and underground foundations, as a powerful prediction tool. Quality control, optimised ingredients and best operational procedures may be achieved by repeatedly simulating the process with different conditions and configurations to ensure high quality of the foundation concrete.

On the basis of continuum equations of fluid and soil mechanics, a comprehensive, versatile, slurry shear model has been developed for transportation of granular grout, paste and fill materials used in the civil and mining industries, covering a wide range of material characteristics and behaviour, namely from the flowing fluid slurries to consolidated solid deposits in underground coal mining induced rock fractures. The theory has been specifically tailor made for grout flows through uniform pipes, discs and tremies, in order to transport material to designated injection or backfill targets. The theory can mimic both flow and blockage behaviour of the fill material. The tool can be used to predict variations of pressure and velocity and their gradients, as a function of flow rate, in the entire backfill-placement system from batching plant to the borehole cracks and foundation excavations.

The shear theory can mimic shear resistance of both: (i) a cohesive, viscous flow and (ii) a stationary, cohesive, pressure-dependent, frictional, plastic soil. The pressure dependent frictional term in the shear stress model determines the frictional resistance of the deposited fill material during a blockage. Consistent with laboratory and field experiments, the theoretical pump pressure required to open a blockage is orders of magnitude greater than the amount needed for pumping the same material when it is under a steady state flow. This explains why very high pump pressures are often needed to clean blockages compared with much lower pressures required during steady state slurry flows.

Concrete flow and placement into deep foundations is normally performed under several harsh environmental conditions of tightness, inaccessibility and deep submergence. Therefore, it must be self compacting, self levelling and maintain its original quality, homogeneity and integrity all the way from the tremie pipe to the discharge point and then through the narrow paths between heavy reinforcements. Traditional slump and spread tests together with the L-box tests are used as indirect index tests to measure physical visco-plastic properties of concrete.

REFERENCES

- Alehossein, H., Poulsen, B. A. 2010, “Stress analysis of longwall top coal caving”. *International Journal of Rock Mechanics and Mining Sciences*, 47(1), 30-1.
- Shen, B. and Alehossein, H. 2009. *ACARP Project C16023, Australia – Subsidence Control Using Coal Washery Waste. An extension research project to ACARP C12019 in 2003 on “Subsidence control using overburden grout injection technology”*.
- Shen, B, Alehossein, H., Poulsen, B., Huddlestone-Holmes, C., Zhou, B., Lou, X., Wang, H., Qin, Z. Duan, J., Jecny, Z, Matt Van de Werken, David Williams - COLLINGWOOD PARK MINE

- REMEDICATION – Subsidence control using fly ash backfilling, *CSIRO Earth Science and Resource Engineering Report July 2010*.
- Alehossein H. 2009, “Viscous, cohesive, non-Newtonian, depositing, radial slurry flow”, *International Journal of Mineral Processing*, V. 93 No. 1, 2009, pp. 11-19.
- Alehossein, H., Shen, B., Qin, Z. and Huddleston-Holmes, C. 2012, “Flow analysis, transportation, and deposition of frictional viscoplastic slurries and pastes in civil and mining engineering.” *Journal of materials in civil engineering*, 24, 644 – 657.
- Alehossein, H., Beckhaus, K. and Larisch, M. 2012, Analysis of L-box tests for tremie pipe concrete. *ACI Materials Journal*, 109 3: 303-311
- Beckhaus, K., Larisch, M., Alehossein, H., Ney, P., Northey, S., Lucas, G., Dux, P., Buttlng, S., Lucas, G., Vanderstaay, L. 2012. Recommended Practice: Tremie Concrete for Deep Foundations”. *Z17, Sept. 2012, Concrete Institute of Australia*.
- Beckhaus, K. and Larisch, M., Alehossein, H., Northey, S., Ney, P., Lucas, G., Vanderstaay L. 2011, “New approach for tremie concrete used for deep foundations”, ICAGE conference, Perth 2011.
- Beckhaus, K. and Larisch, M., Alehossein, H., Northey, S., Ney, P., Lucas, G., Vanderstaay L. 2011, “Performance-based specifications for concrete, 14 – 15 June 2011, Leipzig, Germany.
- M. Larisch, Z. Qin and H. Alehossein. Performance Control Tests and Numerical Simulations for *Concrete in Deep Foundations, 16-18 October, Gold Coast, Queensland, Australia, 2013*.